Molecular & Breeding

A novel regulator of wheat tillering *LT1* identified by using an upgraded BSA method, uni-BSA

Yundong Yuan[1,2] · Bo Lyu[1] · Juan Qi[1] · Xin Liu[1] · Yuanzhi Wang[1] ·
Pierre Delaplace[2] · Yanfang Du[1]

Abstract

Branching/tillering is a critical process for plant architecture and grain yield. However, Branching is intricately controlled by both endogenous and environmental factors. The underlying mechanisms of tillering in wheat remain poorly understood. In this study, we identified *Less Tiller 1* (*LT1*) as a novel regulator of wheat tillering using an enhanced bulked segregant analysis (BSA) method, uni-BSA. This method effectively reduces alignment noise caused by the high repetitive sequence content in the wheat genome. Loss-of-function of *LT1* results in fewer tillers due to defects in axillary meristem initiation and bud outgrowth. We mapped *LT1* to a 6 Mb region on the chromosome 2D short arm and validated a nucleotide-binding (NB) domain encoding gene as *LT1* using CRISPR/Cas9. Furthermore, the lower sucrose concentration in the shoot bases of *lt1* might result in inadequate bud outgrowth due to disturbances in the sucrose biosynthesis pathways. Co-expression analysis suggests that *LT1* controls tillering by regulating *TaROX/TaLAX1*, the ortholog of the *Arabidopsis* tiller regulator *REGULATOR OF AXILLARY MERISTEM FORMATION* (*ROX*) or the rice axillary meristem regulator *LAX PANICLE1* (*LAX1*). This study not only offers a novel genetic resource for cultivating optimal plant architecture but also underscores the importance of our innovative BSA method. This uni-BSA method enables the swift and precise identification of pivotal genes associated with significant agronomic traits, thereby hastening gene cloning and crop breeding processes in wheat.

✉ Yundong Yuan
  yyd2021@outlook.com

✉ Yanfang Du
  yanfangdu@sdau.edu.cn

[1] National Key Laboratory of Wheat Improvement, College of Life Sciences, Shandong Agricultural University, Tai'an 271018, China

[2] Plant Sciences, Gembloux Agro-Bio Tech, University of Liège, Liège, Belgium

 Springer

Introduction

The tillering ability is a crucial agronomic trait that plays a vital role in determining the grain yield of cereal crops, such as it can generate productive tillers that bear grains (Kebrom et al. 2012; Wang et al. 2018a). Breeding programs often optimize tillering to improve crop performance and achieve high yields (Jiao et al. 2010). Wheat (*Triticum aestivum* L.) provides approximately one-fifth of human caloric intake worldwide, highlighting the importance of improving grain yield for global food security (Cao et al. 2020). The mechanisms underlying tillering in wheat remain elusive relative to model species like rice and *Arabidopsis*.

Tillering is known to be regulated by external and internal factors. Tillering/branching involves the initiation of axillary meristems (AMs) and their outgrowth (Yuan et al. 2023). Key genes regulating the process of AM initiation have been identified, such as *MONOCULM1* (*MOC1*) (Li et al. 2003), *LATERAL SUPPRESSOR* (*LAS*) (Greb et al. 2003), *REGULATOR OF AXILLARY MERISTEM FORMATION* (*ROX*) and *LAX PANICLE1* (*LAX1*) (Yang et al. 2012; Komatsu et al. 2003). Bud outgrowth is inhibited in some species by the *TEOSINTE BRANCHED1* (*TB1*) transcription factor and its homologs, which integrate signals from various plant hormones, including strigolactones, auxin, and cytokinins (Wang et al. 2018a; Takeda et al. 2003; Matthes et al. 2019; Kepinski and Leyser 2005; Alder et al. 2012; Smith and Li 2014; Tanaka et al. 2006; Shimizu-Sato et al. 2009).

Emerging evidence highlights the importance of sugars in promoting bud outgrowth, acting as both nutrients and signaling molecules (Mason et al. 2014). For instance, reduced tillering in wheat *tiller inhibition* (*tin*) and rice *monoculm 2* (*moc2*) mutants is attributed to low sucrose levels (Kebrom et al. 2012; Koumoto et al. 2013). Notably, The necessity for sugars for bud outgrowth has been demonstrated in rose (*Rosa hybrida*), where sugar is required to trigger bud outgrowth in single nodes cultivated in vitro (Rabot et al. 2012; Barbier et al. 2015). Sucrose can modulate bud outgrowth dynamics and influence phytohormone homeostasis by stimulating cytokinin biosynthesis and modulating auxin metabolism (Barbier et al. 2015). According to the auxin canalization model, elevated sucrose levels within buds facilitate auxin export, promoting bud outgrowth (Mason et al. 2014; Kebrom and Mullet 2015). These findings collectively demonstrate the crucial role of sugar signaling in regulating bud release.

The rapid development of sequencing technologies in recent years has accelerated the cloning of genes associated with important traits in crops. Traditional forward gene mapping methods, such as map-based cloning, are time-consuming and tedious, especially in wheat with a large and complex genome (17 G) (Consortium et al. 2018). For example, the recent research on the cloned gene *ELS3*, which controls leaf senescence, involved 10,133 individuals and spanned several years (Xie et al. 2023). Current breakthroughs using high-throughput sequencing techniques have accelerated the identification of genes linked to agronomic traits and made gene isolation more feasible and efficient. For instance, the adaptable method MutMap (Abe et al. 2012) has been widely used in identifying genes

associated with a variety of traits, including but not limited to salt tolerance (Takagi et al. 2015), endosperm development (Wang et al. 2018b), flowering and seed size (Manchikatla et al. 2021), height and spikelet (Huang et al. 2022) and more. MutMap-derived methods, such as MutMap + (Fekih et al. 2013), MutMap-Gap (Takagi et al. 2013b), and QTL-seq (Takagi et al. 2013a), have also been developed to improve the efficiency and accuracy of gene mapping. However, the immense wheat genome remains cost-prohibitive for gene cloning using next-generation resequencing data (Consortium et al. 2018). To address the challenge of analyzing the complex wheat genome, the whole-exome resequencing method like BSE-seq has been developed (Dong et al. 2020). This method significantly reduces the amount of data analyzed by focusing on the exome, the protein-coding regions. However, a major hurdle remains: wheat's genome has a remarkably high repetitive sequence content, exceeding 80% (Consortium et al. 2018). This repetitive nature causes short sequencing reads from next-generation sequencing platforms to map to multiple locations in the genome, posing significant challenges for accurately identifying genes. While current Bulk Segregant Analysis (BSA)-based methods, including BSE-seq, MutMap, and others, primarily focus on reducing noise generated by next-generation sequencing platforms, they lack algorithms specifically designed to tackle the noise generated by the inherent high repetitive sequence content of wheat.

Currently, gene cloning in wheat is facing significant challenges. To date, only two genes related to tillering, *Tiller Number1* (*TN1*) (Dong et al. 2023) and the *tiller inhibit* gene (*tin*) (Spielmeyer and Richards 2004), have been successfully isolated using map-based cloning. Most research is focused on reverse genetics, targeted genes such as wheat *TaD27* (Zhao et al. 2020), *TaD14* (Liu et al. 2021), and *TaMOC1* (Zhang et al. 2015). This underscores the urgent need to develop efficient and precise gene cloning methods specifically tailored for wheat. In this study, we upgraded the bulked segregant analysis method called uniquely aligned bulked segregant analysis (uni-BSA), which focuses on reasonably filtering out the reads aligned to multiple positions to increase variant calling accuracy. Through this method, we successfully mapped the wheat '*LESS TILLER1*' (*LT1*) gene to the short arm of chromosome 2D. The candidate *LT1* gene, which encodes a nucleotide-binding domain protein, has been validated through the knockout of *LT1* by CRISPR/Cas9. *LT1* may play a role in regulating tillering through its involvement in auxin, cytokine, and sucrose levels. In summary, we have identified a novel wheat tillering regulator, *LT1*, using the advanced uni-BSA method, which is highly effective for cloning causal genes in wheat. Understanding the role of *LT1* will offer valuable perspectives for molecular breeding in wheat.

Materials and methods

Plant materials and growth conditions

The *lt1* mutant is derived from a mutagenesis pool of a landrace Chang6878 (C6878) treated with 1% Ethyl Methanesulfonate (EMS). The *lt1* phenotypes were

inherited stably after four generations of self-pollination. For gene mapping, *lt1* was backcrossed with C6878 and self-fertilized to produce a segregating F_2 population of at least 1000 individuals. Wheat plants are cultivated in the experimental field at Shandong Agriculture University, Tai'an, Shandong, China. The transgenetic plants are grown in a growth chamber maintained at 22/17°C day/night temperatures, 16-h photoperiod, and about 300 µmol m^{-2} s^{-1} photosynthetically active radiation at 45% humidity.

Exome capture sequencing

Genomic DNAs were extracted from a minimum of 50 individuals with contrasting extreme phenotypes from an F_2 population, along with 10 *lt1* mutants and 10 C6878 plants serving as two control DNA pools, using the CTAB method (Chatterjee et al. 2002). The mutant-type and wild-type DNA pools of the F_2 population were generated by bulking at least 50 genomic DNAs in an equal ratio. The *lt1* mutant and C6878 DNA pools were also generated in an equal ratio.

The datasets generated from Whole-Exome Sequencing (WES) for variation calling in this study were obtained from the Oebiotech company (Shanghai OE Biotech Co., Ltd). In principle, the WES generates 260 Mb of data per fold of the wheat genome, including 110,000 high-confidence protein-coding genes, 50,000 non-coding genes, and associated promoters. We obtained 26 Gb of data per sample, corresponding to 100-fold coverage depth for each gene. For more detailed information on WES and the corresponding bioinformatic pipelines, please refer to the Oebiotech website (https://www.oebiotech.com/).

The uni-BSA pipeline for rapid gene isolation

We developed an enhanced bulked segregant analysis pipeline called uni-BSA for rapid gene cloning in wheat (Fig. 2). This approach consists of the following steps. (1) Develop a segregating population from a backcross between the mutant and the wild-type parental line. (2) Extract and pool DNAs from the mutants, their wild types, and individuals with mutant and wild-type phenotypes of the F_2 population in equal proportions, forming four independent sample pools, respectively. (3) Subject the DNA pools to WES generating deep coverage data (100 folds). (4) Preprocess the raw reads with Fastp (v0.20.1) to remove adapters and low-quality reads (Chen et al. 2018). (5) Align the clean reads to the IWGSC RefSeq v2.1 reference genome using BWA (v0.7.17) mem algorithm with default parameters (Li 2013). (6) Exclude unmapped and non-primary alignments with Samtools view (v1.7) (Li et al. 2009). (7) Use custom Perl script (Filter.ambi.pl supplied as Attachment 1) to process the primary filtered SAM files to retain unambiguous alignments. The main principle is to retain uniquely aligned reads along with their mate reads, even if they are multiply aligned. (8) Remove PCR duplicates and sort the BAM files with Samtools. (9) Use GATK (v4.0.10.1) (McCormick et al. 2015) RealignerTargetCreator and HaplotypeCaller to generate gVCF files, requiring a minimum mapping quality of 30. Use GATK GenomicsDBImport and VariantsToTable to compile variants from all

samples. (10) Use the mean δ-index values (Abe et al. 2012) from 2 Mb sliding windows (0.1 Mb per slide) to define the candidate region. The linkage interval is the region framed by the positions whose corresponding mean δ-index values exceed the 95th percentile of the mean of all δ-index values. (11) Annotate variants using ANNOVAR (Wang et al. 2010) to determine functional effects in coding and non-coding regions.

Construction of CRISPR/Cas9 vector and wheat transformation

To create the vector for gene editing via CRISPR/Cas9, two sgRNAs were designed in the region flanking the *LT1* mutation site by using the CRISPR MultiTargeter web tool (Prykhozhij et al. 2015), targeted on the $CDS^{692-710}$th (target 1: AGTCATATA AACTACATGA) and the $CDS^{919-937}$th (target 2: ATAGTGACAACAAGATCTG) of *LT1*, respectively, and no off-target effects are observed at other positions in the wheat genome. The resulting PCR fragment amplified from the intermediate vector pCBC-MT1T2 was inserted into the binary vector pUBE413 using the "Golden Gate" method (Xing et al. 2014; Dong et al. 2023).

The reconstructed plasmid was introduced into *Agrobacterium* strain EHA105 and transformed into wheat cultivar Fielder. Immature embryo transformation and tissue culture were performed following the protocol described by Sivamani et al. (Ishida et al. 2015). The *LT1* target region was PCR amplified and sequenced to identify mutations (CrLT1-F: GGATTGGGCAAGTCCGAAGA, CrLT1-R: ACC ATCACACCTCCCCACTA) (Table S1). We use three T_2 plants for statistical analysis in every independent transformation event.

Quantification of sucrose content

The quantification of sucrose utilizes acid hydrolysis to break down sucrose into glucose and fructose. The fructose then reacts with phenol to form a colored product that can be detected at a 480-nm wavelength. Shoot base samples were harvested from 30 individuals of *lt1* mutants and wild-type C6878 at the developmental stages of two, three, and four leaves, with three biological replicates per stage. Approximately 100 mg of fresh shoot base tissue was ground in liquid nitrogen for each sample. Sucrose extraction and colorimetric detection were performed following the detailed protocol provided in the sucrose assay kit from Solarbio (item no. BC2465).

Dynamic observation of AM development and its subsequent outgrowth in wheat

To evaluate AM development in wheat, seedlings were examined at the developmental stages of 1) only coleoptile emerged, 2) two leaves, and 3) four leaves. At each stage, shoot base samples were collected randomly from several seedlings. After carefully removing the leaves, the shoot bases were directly visualized using a stereomicroscope. The number of visible axillary meristems was counted at each timepoint. We also examined the plants after the heading stage for axillary bud

outgrowth to observe if they had ceased axillary buds, like the process of AM number counting.

Co-expression analysis

Tissues used in gene expression analysis were harvested from shoot bases where AMs arise. These materials belong to *lt1* and C6878 at three different development stages: 2-leaf, 3-leaf, and 4-leaf stages, with three replicates per time point. mRNA for each sample was extracted using TRIzol Reagent (Invitrogen) and then subjected to RNA sequencing performed by the ANOROAD company. Clustering analysis was performed using the Mfuzz R package (Kumar and Futschik 2007). The data containing all sample Transcripts Per Million Mapped Reads (TPM) values was first standardized using z-score normalization. Soft clustering was then carried out using the "mfuzz" R package with default parameters. Differentially expressed genes (DEGs) were identified using the R package DEGseq2 (Love et al. 2014). Genes with absolute $\log_2$ fold change greater than one and adjusted p-value (padj) less than 0.05 relative to the wild-type plant were considered statistically significantly expressed. Gene ontology (GO) analysis was conducted to categorize DEGs into functional groups. The GO annotation library for each wheat gene was calculated from the eggNOG database (version 4.5) using default parameters (Huerta-Cepas et al. 2019). These annotations were then used to build a custom R package, "*org.Taestivum.eg.db*", containing the GO information for all genes analyzed. The R package clusterProfiler (Wu et al. 2021) was utilized along with "*org.Taestivum. eg.db*" to perform GO enrichment analysis on DEGs. Details on the use of cluster-Profiler can be found in its documentation.

Subcellular localization assay

To investigate the subcellular localization of the LT1 protein, we performed an in vitro localization experiment using wheat protoplasts. We fused the C-terminal of LT1 from the Chinese Spring wheat landrace to GFP plasmid pBL21 and transformed the fusion construct LT1-GFP into wheat protoplasts via polyethylene glycol-mediated transfection, as described previously by Xiong et al. (2022) (Xiong et al. 2022). After incubating transformed protoplasts at 23°C for 12–16 h, we visualized GFP fluorescence by confocal laser scanning microscopy (LSM 880, Carl Zeiss, Germany) to determine the intracellular localization of the LT1-GFP protein.

Quantitative RT-PCR

Quantitative real-time PCR (qRT-PCR) was performed to assess gene expression levels, as described previously (Xiong et al. 2022). Briefly, total RNA was extracted using TRIzol Reagent (Invitrogen), followed by DNase I (Takara) treatment to remove residual DNA, and then the RNA was purified using an RNA purification kit (Tiangen). First-strand cDNA synthesis was carried out using the iScript cDNA synthesis kit (Bio-Rad). qRT-PCR was conducted using the SsoFast EvaGreen

Supermix kit (Bio-Rad) on a CFX 96 real-time PCR system (Bio-Rad) with the following amplification program: 95°C for 2 min, 40 cycles of 95°C for 5 s, and 60°C for 35 s. Primers used for qRT-PCR are listed in Supplemental Table S1. The wheat *ACTTIN* (*TraesCS1A02G020500*) (Tables1) gene served as an internal control. Relative gene expression was calculated by the $2^{-\Delta\Delta Ct}$ method (Livak and Schmittgen 2001). Each experiment was performed with at least three biological replicates.

Results

Phenotypes of the wheat tillering mutant *lt1*

The *lt1* mutant was derived from an EMS mutagenesis pool of the elite wheat landrace C6878. This recessive mutant exhibits reduced tillering, typically producing four tillers compared to eighteen of C6878 at the heading stage (Fig. 1A-B). Additional pleiotropic defects in *lt1*, including decreased stature, short roots, chlorotic leaves, and wrinkled seeds, are concomitant (Fig. S1). To explain whether the reduced tillers are due to defects in bud initiation or bud elongation, we observed the dynamic development process of tiller buds. At first, we found that the number of AMs remained consistent during the coleoptile and two-leaf stages but started to diverge by the four-leaf stage, with four in the wild type and two in *lt1* (Fig. 1C-D). This revealed that the reduced tillering of *lt1* is partially due to the defective AM initiation. Furthermore, we examined the number of ceased lateral buds at the heading stage. A lower ratio of ceased lateral buds (Ratio=Ceased buds/all buds) in *lt1* compared to C6878 indicated that the tiller buds were negatively regulated during tiller bud outgrowth stages in *lt1*(Fig. 1E-F). Taken together, the tillering defect of *lt1* appears attributable to both its reduced AM formation and bud outgrowth.

Isolation of *LT1* by an upgraded bulked segregant method, uni-BSA

We backcrossed *lt1* to its parental line C6878 and performed self-crossing to generate the F_2 segregating population. All the F_1 individuals showed comparable tiller numbers as C6878, indicating that *lt1* has a recessive mutation. The low-tillering plants (one to four tillers) compared to the high-tillering plants (over 15 tillers) in the F_2 generation fit the Mendelian of 3:1 ratio (710 multi-tillering plants:205 low-tillering plants, $\chi^2=1.6367$, p=0.2008). These results suggest that a recessive single gene controls the *lt1* mutant.

To expedite the cloning of *LT1*, we utilized the BSA-based method uni-BSA, using the sequence data from WES, making it cost-friendly and effective. Firstly, the WES data was used to minimize the genome size without the penalty of losing protein-encoding genes while guaranteeing enough SNPs to carry out linkage analysis. Secondly, to address the ambiguous mapping when alignment is performed due to the high duplication proportion of the wheat genome, which may result in aligning one read to multiple loci, we tailor-make a Perl script called Filter.ambi.pl integrated into the uni-BSA protocol (Fig. 2). The principle
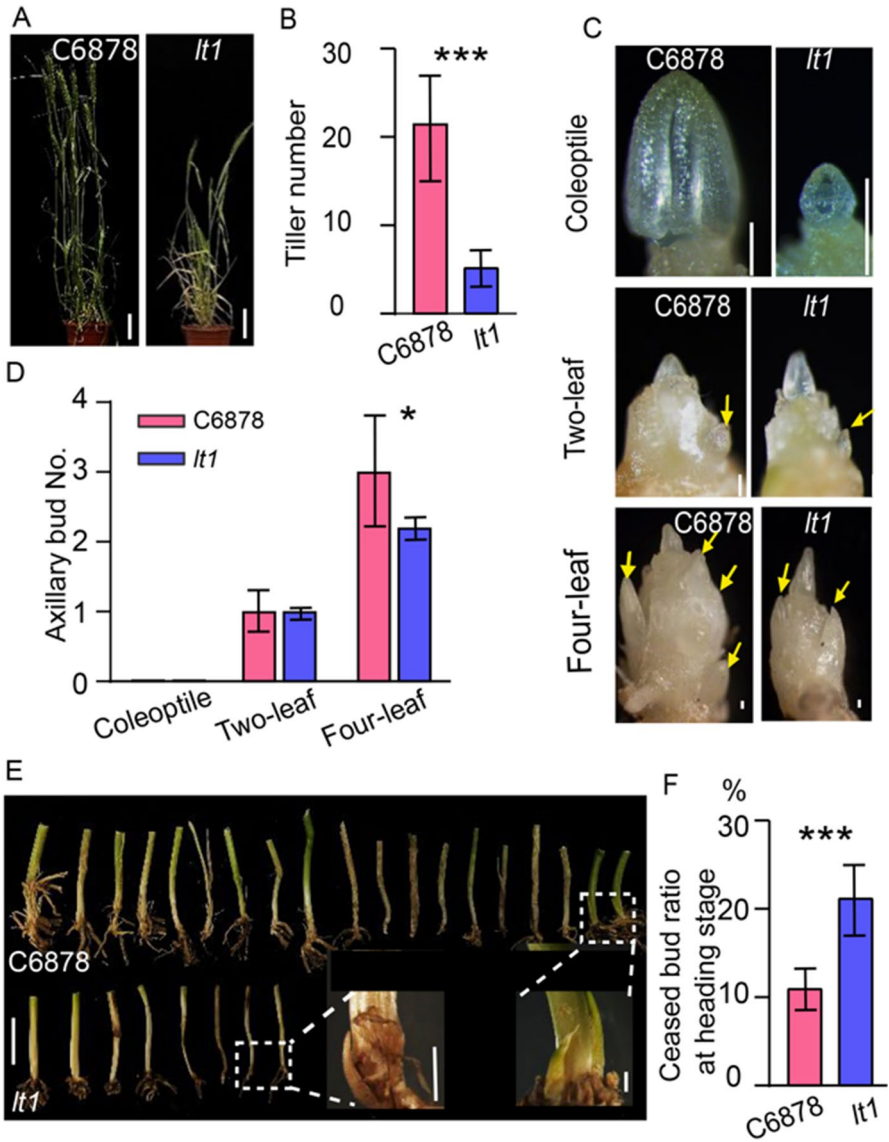
Fig. 1 Phenotypes of *lt1*. (**A**) Tiller number comparison between *lt1* and C6878. Bar = 15 cm. (**B**) The statistical values representing the tiller number of *lt1* and C6878. Values are means ± SD (n = 10). *** P < 0.001, Student's t-test. (**C**) Dynamic observation of AM formation between *lt1* and C6878, namely, coleoptile, two- and four-leaf stages. The yellow arrow indicates the bud primordium. Bar = 200 μm. (**D**) Axillary bud number of *lt1* and C6878 at each stage. Values are means ± SD (n = 5). * P < 0.05, Student's t-test. (**E**) Ceased bud observation at the heading stage. The ceased buds are closed up in the white box. Bar = 1 cm. (**F**) Ceased bud ratios at the heading stage. Values are means ± SD (n = 4). ** P < 0.01, Student's t-test
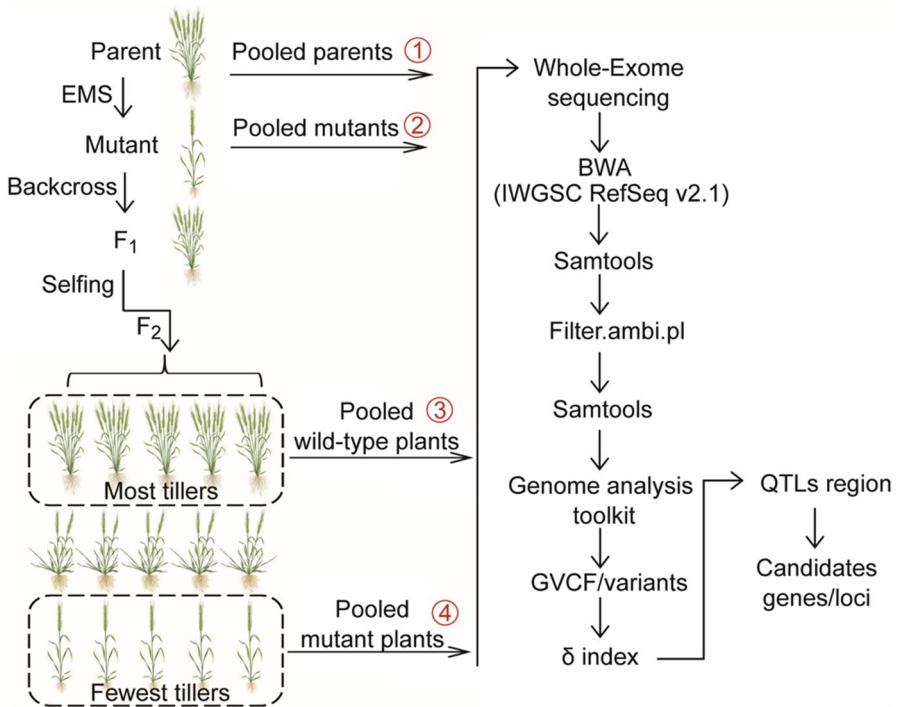
Fig. 2 Pipeline of the enhanced BSA method. In this flowchart, seeds of wheat C6878 were mutagenized by EMS. The M_2 or higher generation mutant plant of *lt1* was backcrossed to C6878 and self-pollinated to generate an F_2 segregating population. Four bulks indicated by red circled digits were subjected to Whole-Exone sequencing (WES). The big datasets were aligned against the Chinese Spring version 2.1. Then, the resulting sam files were primarily filtered and deep processed by the Perl script "Filter.ambi.pl" to leverage as more as possible reads. Sequentially, the GVCF files containing all variants were generated. The causal variants responsible for the mutant phenotype were identified in the candidate interval

of our filtering algorithm is based on the fact that one DNA fragment generates two sequences: a forward sequence and a reverse sequence. If either of these sequences aligns to one position, its mate should be nearby, regardless of whether it aligns to multiple sites (Fig. S4A). Discarding sequences with uniquely aligned mate reads, as done in strict filtering methods, is inefficient. Our algorithm, Filter. ambi.pl, addresses this by retaining such sequences, resulting in broader genome coverage (Fig. S2A) in comparison to the strict filtering method. Accordingly, this filtering method retained 61% of total reads, compared to 48% when discarding all ambiguous reads (Fig. S2B). The average percentage of each gene coverage was over 81%, with the majority of genes covered at 100% (Fig. S2C). The average coding sequencing depth reached 70X (Fig. S2D). Notably, this algorithm produces more accurate variants compared to the no-filtering method (Table S3). For example, a mutation site (C-T) identified by the no-filtering method is heterozygous. Collectively, the filtering algorithm of uni-BSA is powerful and efficient.
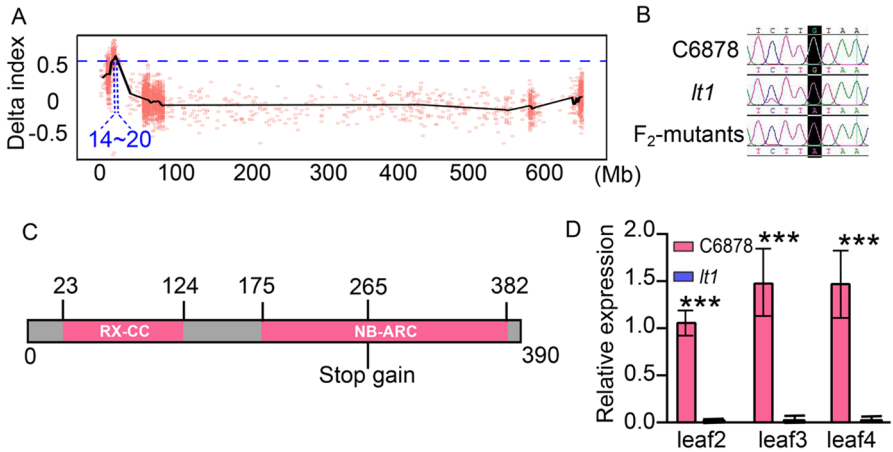
Fig. 3 Gene cloning of *LT1*. (**A**) Gene linkage analysis. It indicates that *LT1* is framed in a 6 Mb interval on the short arm of the chromosome 2D between 14–20 Mb. The horizontal dotted line represents the 95th mean of all the delta indexes. (**B**) Mutation validified by Sanger sequencing. The nucleotide change is shaded. Individuals in the F_2 population with the homozygous mutation display *lt1* phenotypes. (**C**) Schematic diagram of LT1. This protein contains an RX-CC (N-terminal coiled-coil) domain and the NB-ARC (nucleotide-binding domain) domain. The stop gain position is at the 265th amino acid. (**D**) Relative expression of *LT1* at three stages of *lt1* and the C6878. Values are means $\pm$ SD (n = 3). *** P < 0.001, Student's t-test

Uni-BSA application narrowed *LT1* to a 6 Mb region on the short arm of chromosome 2D (Fig. 3A), compared to 8 Mb without ambiguous read filtering (Fig. S4D). This interval contains 140 genes, of which 65 genes have variations, including SNPs and Indels. We excluded genes with heterozygous variants in the fewest-tillering pooled DNA samples, remaining 26 genes. Since EMS predominantly causes SNPs rather than Indels, we excluded 14 Indels, thereby eliminating 9 genes. We also excluded 12 genes containing 28 SNPs in *lt1* that matched the reference Chinese Spring, which exhibits normal tillering. Ultimately, five genes were identified as candidate genes (Table S2, Attachment 2). Interestingly, one gene, *TraesCS2D03G0082100*, encoding a nucleotide-binding (NB) domain protein (Fig. 3C), harbors an SNP mutation in the 793rd base (C-T), causing a premature of this gene in *lt1* (Fig. 3C), while the other four genes had UTR mutations (Table S2). In addition, the individuals of the F_2 population with this homozygous mutation (Fig. 3B) show *lt1* phenotypes. Further, *TraesCS2D03G0082100* was not expressed in 2-leaf, 3-leaf, and 4-leaf stages of *lt1*, compared to the wildtype (Fig. 3D). We initially considered *TraesCS2D03G0082100* the likely causal *LT1* gene, given its severe mutation and undetectable expression.

Verification of *LT1*

To validate *TraesCS2D03G0082100* as the *LT1* gene regulating tillering in wheat, we used CRISPR/Cas9 to create knock-out mutants in the wheat cultivar
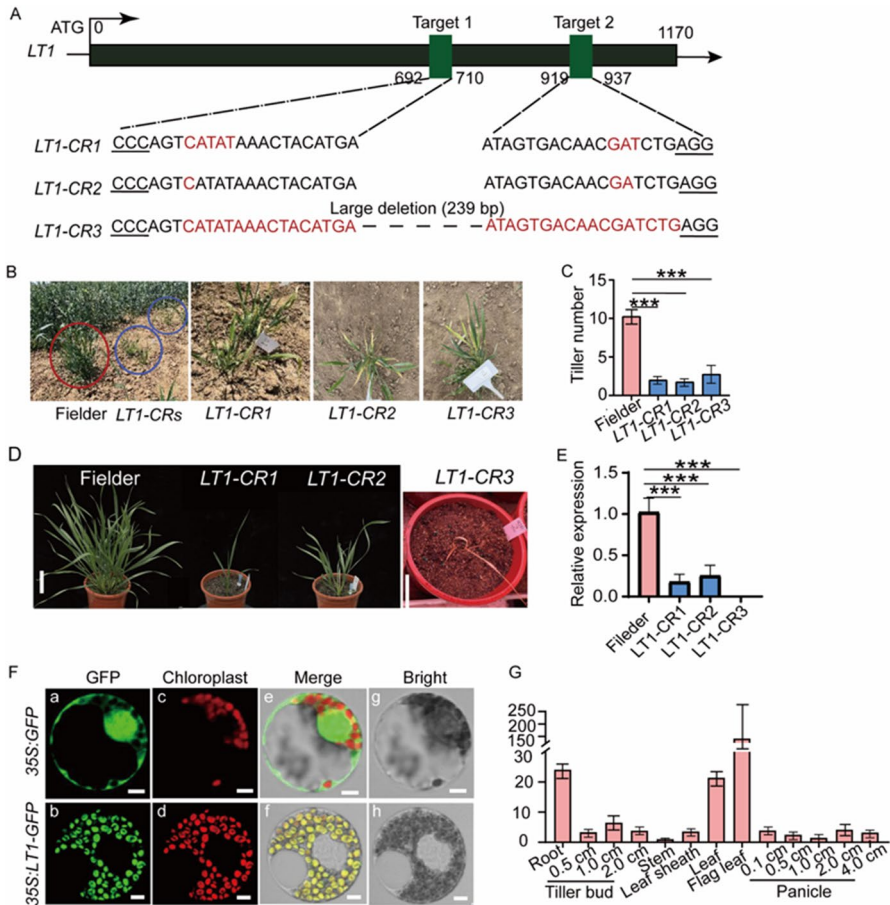
Fig. 4 Verification of *LT1*. (**A**) Schematic diagrams indicating targets of CRISPR/Cas9 (*LT1-CRs*) and the mutations in each line. PAM sites are depicted with underlines. Deletions are indicated with words in red color, and *LT1-CR3* had a 293 deletion. (**B**) Phenotypes of *LT1-CRs*. All the *LT1-CRs* show *lt1* phenotypes, including yellow leaves and fewer tillers in the field conditions. The wild-type plants circled by red are Fielder. The *LT1-CRs* are boxed by blue circles and closed up in the right pictures. (**C**) Tiller number comparison between *LT1-CRs* and the wild type. Values are means ± SD (n = 3). *** P < 0.001, Student's t-test. (**D**) Phenotypes of *LT1-CRs* in the cabinet. Progenies of *LT-CR1* and *LT-CR2* grown in the growth cabinet at the seedling stage show fewer tillers. Progenies of *LT-CR3* are lethal in seedlings. Bar = 7.5 cm. (**E**) Relative expression levels of *LT1* in *LT1-CRs* and Fielder. The values are relative to *ACTIN*. Values are mean ± SD (n = 4). *** P < 0.001, Student's t-test. (**F**) Sublocation of LT1 using wheat protoplasts. Scale bars correspond to 10 μm. (**G**) Relative expression levels of *LT1* in various tissues. The values are relative to *ACTIN*. Values are mean ± SD (n = 3)

Fielder. The three independent edited lines with different mutations within its coding sequences were obtained (Fig. 4A). The *LT1-CR1* and *LT1-CR2* show the mutations at gRNA targeted sites, and *LT1-CR3* has 239 bp deletion (Fig. 4A). Intriguingly, all three edited homozygous individuals produced fewer tillers than the wild type in both field and greenhouse experiments, and reduced expression

level of *LT1* (Fig. 4B-E). Moreover, these three lines exhibit other defects of *lt1,* like yellow leaves (Fig. 4B, D), thus confirming *TraesCS2D03G0082100* as the *LT1* locus.

To elucidate the possible reasons for pleiotropic phenotypes of the *lt1* mutant, we assessed the expression levels of *LT1* in various tissues. qPCR analysis revealed ubiquitous expression of *LT1*, with exceptionally high levels in leaves (Fig. 4G). Given its high level in leaves, it is not strange that *lt1* has yellow leaves once *LT1* is disrupted. *LT1* was detectable in tiller buds, albeit at relatively lower levels (Fig. 4G). The broad expression pattern of *LT1* suggests its multiple roles in wheat development. Overall, these data indicate that *LT1* likely influences tillering and other developmental processes directly or indirectly.

To determine the sublocation of LT1, we carried out a transient expression experiment of LT1 in wheat protoplasts. In contrast with the control, which is ubiquitous in protoplast cells, the LT1-GFP fusion protein was predominantly localized in chloroplasts (Fig. 4F). The chloroplast location of LT1 implies that *LT1* may operate nutrition production, like sucrose, to control tillering.

The regulatory pathways of *LT1* in tillering development

LT1 controls lateral bud formation by targeting *TaROX/TaLAX1* directly or indirectly

To further investigate modular relationships involving *LT1*, we conducted a co-expression analysis using TPM values from shoot base tissues at three developmental stages: the two-leaf, three-leaf, and four-leaf stages. An initial survey of these RNA-seq datasets revealed that samples belonging to each group clustered well (Fig. S3). By analyzing the TPM values of C6878, the transcripts were grouped into eight clusters, each representing distinct gene expression trends (Fig. 5A). *LT1* expression, which belongs to cluster five, was highest at the 2-leaf stage and then decreased at the three- and four-leaf stages. We considered the 2-leaf stage to be crucial for AM initiation, as genes active at this stage showed a peak in expression, followed by a decrease in the subsequent stages. Therefore, we performed GO analysis on genes within the overlap between cluster five and the 2-leaf stage (Fig. 5B), which showed significant expression changes between *lt1* and C6878 (absolute log2FoldChange > 1, FDR < = 0.05). This analysis revealed perturbations in various pathways in *lt1*. Notably, in this stage, various pathways (Fig. 5C) related to AM formation shared the locus *TraesCS3B02G383000*, an ortholog of *Arabidopsis ROX* and *LAX1* in rice that regulate AM formation. These pathways include "morphogenesis of a branching structure", "secondary shoot formation", and "shoot axis formation". Moreover, *TraesCS3B02G383000*, namely *Ta3BLAX1,* is undetectable in *lt1* (Fig. 5D). This is consistent with our previous observation of significant differences in tiller numbers at the four-leaf stage in *lt1* mutants (Fig. 1C). Taken together, *LT1* might regulate AM initiation by affecting *TaROX/TaLAX1* directly or indirectly.
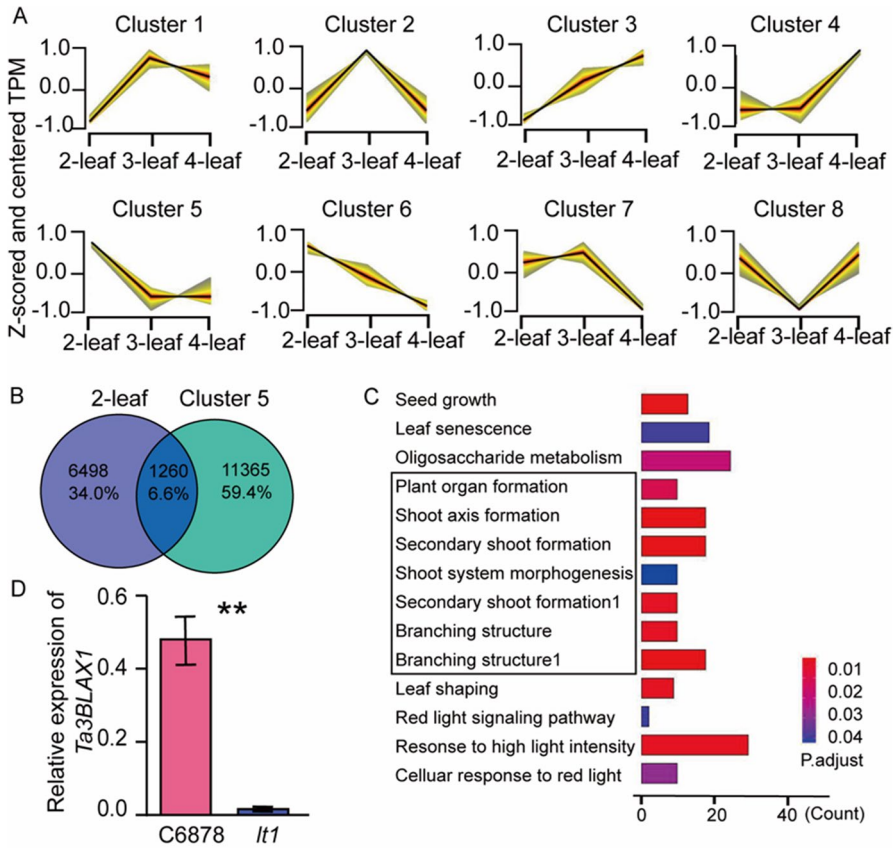
Fig. 5 Co-expression analysis of DEGs in C6878 and *lt1*. (**A**) Eight clusters of all the gene expression are grouped distinctly. The cluster 5 contains *LT1*. (**B**) Venn diagram showing the proportion of overlapped genes between the leaf2 stage (significantly changed) and cluster 5. (**C**) Go analysis of the genes belonging to the intersection between the leaf 2 stage and cluster 5 containing *LT1*. Pathways sharing *TaLAX1* are framed by the black box. P. adjust values indicating significance are colored gradually from blue to red. (**D**) Expression levels of *Ta3BLAX1*. Values are mean ± SD (n = 4). ** P < 0.01, Student's t-test

Auxin and cytokinin are involved in tiller development in *lt1*

Auxin and CK play antagonistic roles in regulating tillering (Yuan et al. 2023). We performed GO analysis on the genes in the intersection between the three developmental stages and cluster 5, respectively. The results revealed perturbation in several phytohormone-related pathways, including auxin, CK, salicylic acid, and jasmonic acid (Fig. 6A). Among these pathways, the indole-containing compound biosynthesis process, in which auxin is biosynthesized, was enriched at all three developmental stages. For example, TrpA family genes *Ta5BTrpA* and *Ta5DTrpA* exhibited significant upregulation in *lt1*. This suggests that higher auxin levels may inhibit tillering in *lt1* (Fig. 6B). In addition to auxin, CK levels
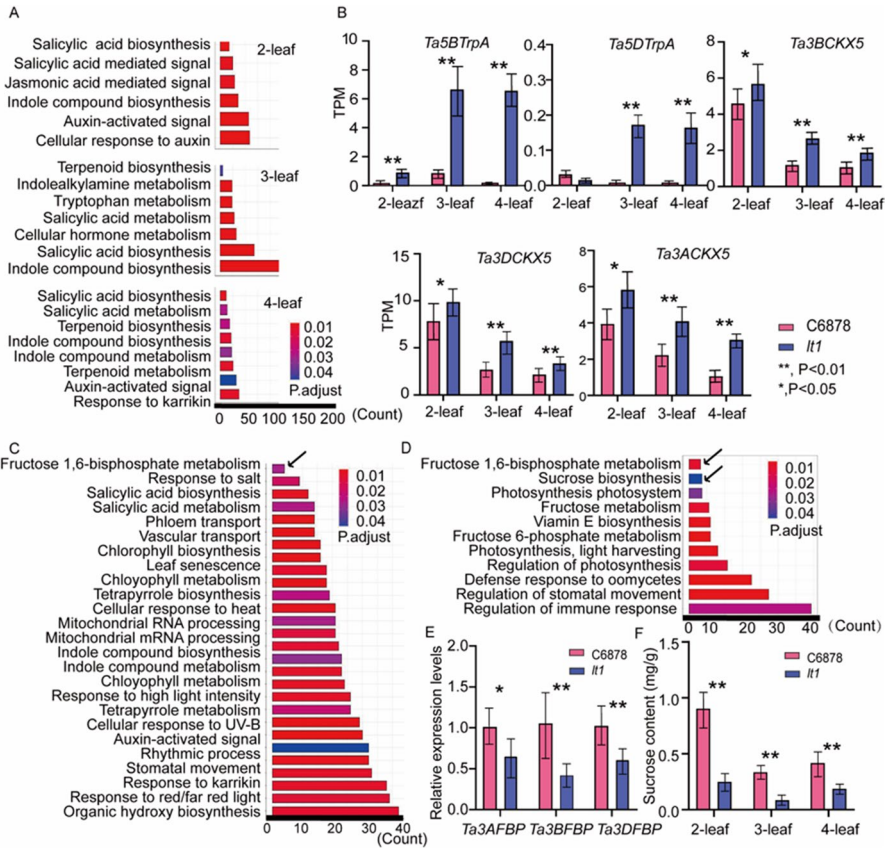
Fig. 6 GO analysis of genes related to auxin, cytokinin, and sucrose. (A) Various phytohormones enriched by GO analysis. The P.adjust values are portrayed by blue to red gradient colors. The gene number represented by values on the X-axis is the count number belonging to the pathways enriched. (B) Auxin and cytokinin related gene expression (TPM) values. Values are means $\pm$ SD (n=3). *** P<0.001, Student's t-test. (C) and (D) Go analysis of DEGs at the four-leaf stage and DEGs from seedlings. The sucrose biosynthesis pathways perturbed are arrowed. The gene number represented by values of the X-axis is the count number belonging to the pathways enriched. P.ajust values indicating significance are colored gradually from blue to red. (E) Relative expression levels of *FBPase*. The Values are relative to *ACTIN*. (F) Sucrose content comparison. Sucrose levels of *lt1* in three developmental stages are all reduced significantly than that in C6878. Values are means $\pm$ SD (n=3). *** P<0.001, Student's t-test

were suggestively decreased, as indicated by the upregulation of *TaCKX5* (*cytokinin dehydrogenase 5*) genes (*Ta3ACKX5, Ta3BCKX5, and Ta3DCKX5*) mediating CK degradation (Fig. 6B). These *CKX5* genes were also enriched in pathways related to secondary shoot formation (Bartrina et al. 2011), implying CK metabolism may play an important role in *lt1* deficient mutant. Taken together, *LT1* may regulate tillering through the involvement of auxin and cytokinin-related pathways.

LT1 may function through the sucrose biosynthesis pathway

As with all organisms, plants require energy for growth. They achieve this by intercepting light and fixing it into usable chemical forms via photosynthesis. The resulting carbohydrate (sugar) energy is then utilized as substrates for growth or stored as reserves (Eveland and Jackson 2012), thus influencing various aspects of plant development, such as tillering (Rabot et al. 2012). Our co-expression analysis revealed perturbations in the fructose 1,6-bisphosphate (FBP) pathway at the four-leaf stage, which is involved in sucrose biosynthesis (Fig. 6C). Coincidentally, RNA-seq analysis using whole seedlings with two leaves also showed perturbations of the FBP pathway genes (Fig. 6D). Within this pathway, three closely related *TaFBPase* genes involved in sucrose biosynthesis were down-regulated in *lt1* mutants (Fig. 6E), implying lower sucrose levels. To determine if the sucrose levels have changed in the *lt1* mutant, we collected the shoot base at the two-, three-, and four-leaf stages and measured the sucrose level. Indeed, it decreased significantly in *lt1* mutants compared to wildtype (Fig. 6F). Together, these datasets suggest *LT1* may exert its influence on tillering and other phenotypes by targeting *FBPases*, thereby impacting sucrose levels.

Discussion

In higher plants, the degree and pattern of tillering/branching are major determinants of plant architecture and grain yield, especially in crops. Significant advances have been made in identifying genes controlling branching in model plants like *Arabidopsis* and rice, but fewer genes controlling tillering have been identified in wheat. This study used a new approach called uni-BSA to clone *LT1*, a chloroplast protein with an NB-containing domain. Functional analysis revealed that *LT1* modulates auxin, CK, and sucrose levels to control tillering in wheat (Fig. 7).

Fig. 7 A proposed model of *LT1* regulating tillering. In this model, *LT1* promotes *TaLAX1* to regulate AM formation. *LT1* can affect *TaFBPase* expression levels, thus mediating internal sucrose content to facilitate axillary bud outgrowth. *LT1* also impacts phytohormone-related genes to control tillering, as it inhibits *TrpA* to reduce auxin levels and inhibits *TaCKX5s* to increase cytokinin levels
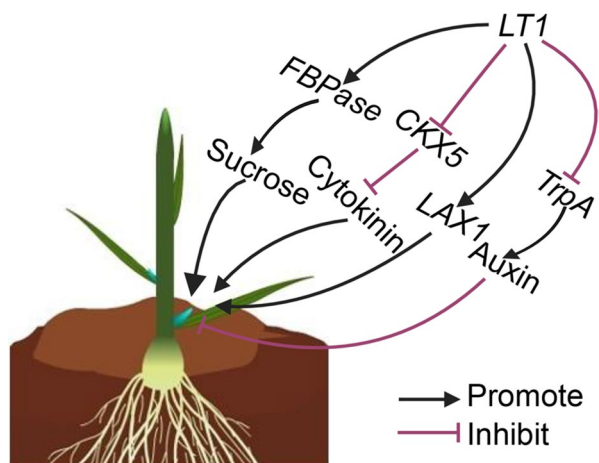
The uni-BSA method is well-suited for wheat gene cloning

BSA is a cost-effective and robust approach for identifying causal genes from segregating populations. BSA-based methods, such as bulked segregant RNA sequencing (BSR-seq) (del Viso et al. 2012), Mutmap (Abe et al. 2012), and Graded-seq (Wang et al. 2019), enable the rapid development of genetic markers and gene cloning. However, few genes have been mapped using BSA-based methods in wheat. This is mainly due to the high cost of whole genome resequencing for BSA, which becomes prohibitive given the large genome size of wheat and the high proportion of repetitive regions that lead to ambiguous read mapping. To address these challenges, firstly, we implemented WES to identify variations while ensuring sufficient markers for the linkage analysis and, thus, reducing the genome from 17 Gb to 260 Mb. A similar approach like BSE-seq (Dong et al. 2020) using WES data with the varB-score algorithm has successfully cloned several genes. However, it did not address the issue of high repetitive sequence content inherent in the wheat genome. We developed an effective uni-BSA algorithm to filter ambiguous reads while retaining as many reads as possible, improving mapping accuracy and narrowing down smaller candidate gene intervals (Fig. S4D). Namely, uni-BSA can produce more sensitive δ index values than those with no-filtering or strict-filtering methods, making it easier to define linkage areas (Fig. S4C). While the linkage interval defined by the strict-filering method is same as uni-BSA, the uni-BSA covers more genomic areas by using its algorithm (Fig. S2A). Additionally, this algorithm produces more accurate variants compared to the no-filtering method (Table S3). For example, a mutation site (C-T) identified by the no-filtering method is heterozygous. Collectively, our uni-BSA method is a powerful and preferable approach for gene cloning in wheat.

LT1 shares an NB domain with plant resistance proteins

The NB domain is a common feature of many plant resistance proteins, also known as NB-LRR proteins, named after their central NB domain and C-terminal leucine-rich repeat (LRR) domain (Takken and Tameling 2009). Because R proteins can trigger host cell death, their activity requires tight regulation. Studies of R protein interactions and mutagenesis revealed that both the NB and LRR domains play a role in the auto-inhibition of these proteins (Rairdan and Moffett 2006, 2007). Additionally, the LRR domain likely functions in recognizing avirulence effectors produced by pathogens (Takken and Tameling 2009). Despite their role in disease resistance, dysregulation of R proteins also impacts developmental processes, resulting in phenotypes like stunted dwarfism (Yang and Hua 2004; Michael Weaver et al. 2006), increased branching (Igari et al. 2008), early leaf senescence (Xie et al. 2023), altered plant height (Borrill et al. 2022), and abnormal panicle development (Pan et al. 2022).

Unlike other R proteins, the *LT1* gene identified in our study encodes only an NB domain, lacking the LRR domain. Our analysis showed 2035 NB domain-containing

genes in the wheat genome, with 964 lacking LRR domains (Fig. S5). The evolutionary mechanisms leading to the high number of NB-only proteins require further investigation. We hypothesize that disruption of *LT1* removes its auto-inhibition, thereby activating resistance responses and impacting developmental pathways like tillering. Alternatively, *LT1* may presumably play a direct role in the regulation of tillering, independent of disease resistance.

The chloroplast location of LT1 provides a link between its effect on disease resistance and plant development. Chloroplasts are energy production sites, so localization to this organelle implies that LT1 may impact developmental processes by influencing energy production. This is consistent with the pleiotropic phenotypes observed in *lt1*, such as reduced tillering, plant height, and short roots. Further investigation of how a chloroplast-localized protein like LT1 influences energy production and downstream developmental pathways will shed important light on its roles in plant growth and disease resistance.

LT1 is essential in controlling wheat developments, especially in tillering

Crop tillering is a trait closely related to yield. *LT1* is a new gene controlling wheat tiller number through both disrupting bud initiation and its outgrowth. CRISPR/Cas9-generated transformants phenocopied *lt1* phenotypes, including reduced tiller number, shorter stature, yellow leaves, and additional traits. However, some progeny derived from certain heterozygous individuals, especially those with large truncations of *LT1*, like *LT-CR3*, displayed lethal phenotypes in seedlings (Fig. 4D), as evidenced by yellowing and withered leaves. This seedling lethality in some genotypes likely explains the inability to find lines exhibiting *lt1* phenotypes in segregating populations in the field conditions, as these lines died at early developmental stages. Overall, the pleiotropic effects caused by *LT1* disruption, including lethality in severe cases, demonstrate that *LT1* plays an essential role in regulating diverse aspects of wheat development.

In our study, we observed significant alterations in sucrose levels and phytohormone metabolism throughout the dynamic developmental stages of *lt1* (Fig. 7). Notably, *LT1* is also shown to influence the *TaROX/TaLAX1* gene, a key mediator of axillary meristem initiation. Together, these results provide new insights into the molecular mechanisms governing tillering in wheat. Elucidation of *LT1*'s multifaceted roles in this process, from energy metabolism to hormone signaling, will enable more targeted breeding efforts to optimize tiller number and wheat yields. Further exploration of *LT1* and its interacting partners will enhance our understanding of the intricate regulatory systems that will illuminate the complex regulatory networks controlling tillering and plant architecture in cereal crops.

Declarations

Ethics approval and consent to participate Not applicable.

Consent for publication Not applicable.

Competing interests The authors declare no competing interests.

References

Abe A, Kosugi S, Yoshida K, Natsume S, Takagi H, Kanzaki H, Matsumura H, Yoshida K, Mitsuoka C, Tamiru M, Innan H, Cano L, Kamoun S, Terauchi R (2012) Genome sequencing reveals agronomically important loci in rice using MutMap. Nat Biotechnol 30(2):174–178. https://doi.org/10.1038/nbt.2095

Alder A, Jamil M, Marzorati M, Bruno M, Vermathen M, Bigler P, Ghisla S, Bouwmeester H, Beyer P, Al-Babili S (2012) The path from β-carotene to carlactone, a strigolactone-like plant hormone. Science 335(6074):1348–1351. https://doi.org/10.1126/science.1218094

Barbier F, Péron T, Lecerf M, Perez-Garcia M-D, Barrière Q, Rolčík J, Boutet-Mercey S, Citerne S, Lemoine R, Porcheron B (2015) Sucrose is an early modulator of the key hormonal mechanisms controlling bud outgrowth in *Rosa hybrida*. J Exp Bot 66(9):2569–2582. https://doi.org/10.1093/jxb/erv047

Bartrina I, Otto E, Strnad M, Werner T, Schmülling T (2011) Cytokinin regulates the activity of reproductive meristems, flower organ size, ovule formation, and thus seed yield in *Arabidopsis thaliana*. Plant Cell 23(1):69–80. https://doi.org/10.1105/tpc.110.079079

Borrill P, Mago R, Xu T, Ford B, Williams SJ, Derkx A, Bovill WD, Hyles J, Bhatt D, Xia X (2022) An autoactive *NB-LRR* gene causes *Rht13* dwarfism in wheat. Proc Natl Acad Sci U S A 119(48):e2209875119. https://doi.org/10.1073/pnas.2209875119

Cao S, Xu D, Hanif M, Xia X, He Z (2020) Genetic architecture underpinning yield component traits in wheat. Theor Appl Genet 133(6):1811–1823. https://doi.org/10.1007/s00122-020-03562-8

Chatterjee A, Moulik S, Majhi P, Sanyal S (2002) Studies on surfactant–biopolymer interaction I. microcalorimetric investigation on the interaction of cetyltrimethylammonium bromide (CTAB) and sodium dodecylsulfate (SDS) with gelatin (Gn), lysozyme (Lz) and deoxyribonucleic acid (DNA). Biophys Chem 98(3):313–327. https://doi.org/10.1016/s0301-4622(02)00107-2

Chen S, Zhou Y, Chen Y, Gu J (2018) Fastp: an ultra-fast all-in-one FASTQ preprocessor. Bioinformatics 34(17):i884–i890. https://doi.org/10.1093/bioinformatics/bty560

Consortium IWGS, Appels R, Eversole K, Stein N, Feuillet C, Keller B, Rogers J, Pozniak CJ, Choulet F, Distelfeld AJS (2018) Shifting the limits in wheat research and breeding using a fully annotated reference genome. Science 361(6403):eaar7191. https://doi.org/10.1126/science.aar7191

del Viso F, Bhattacharya D, Kong Y, Gilchrist MJ, Khokha MK (2012) Exon capture and bulk segregant analysis: rapid discovery of causative mutations using high-throughput sequencing. BMC Genomics 13:1–11. https://doi.org/10.1186/1471-2164-13-649

Dong C, Zhang L, Chen Z, Xia C, Gu Y, Wang J, Li D, Xie Z, Zhang Q, Zhang X, Gui L, Liu X, Kong X (2020) Combining a new exome capture panel with an effective varBScore algorithm accelerates BSA-based gene cloning in wheat. Front Plant Sci 11:1249. https://doi.org/10.3389/fpls.2020.01249

Dong C, Zhang L, Zhang Q, Yang Y, Li D, Xie Z, Cui G, Chen Y, Wu L, Li Z, Liu G, Zhang X, Liu C, Chu J, Zhao G, Xia C, Jia J, Sun J, Kong X, Liu X (2023) *Tiller Number1* encodes an ankyrin repeat protein that controls tillering in bread wheat. Nat Commun 14(1):836. https://doi.org/10.1038/s41467-023-36271-z

Eveland AL, Jackson DP (2012) Sugars, signalling, and plant development. J Exp Bot 63(9):3367–3377. https://doi.org/10.1093/jxb/err379

Fekih R, Takagi H, Tamiru M, Abe A, Natsume S, Yaegashi H, Sharma S, Sharma S, Kanzaki H, Matsumura H, Saitoh H, Mitsuoka C, Utsushi H, Uemura A, Kanzaki E, Kosugi S, Yoshida K, Cano L, Kamoun S, Terauchi R (2013) MutMap+: genetic mapping and mutant identification without crossing in rice. PLoS ONE 8(7):e68529. https://doi.org/10.1371/journal.pone.0068529

Greb T, Clarenz O, Schafer E, Muller D, Herrero R, Schmitz G, Theres K (2003) Molecular analysis of the *LATERAL SUPPRESSOR* gene in *Arabidopsis* reveals a conserved control mechanism for axillary meristem formation. Genes Dev 17(9):1175–1187. https://doi.org/10.1101/gad.260703

Huang X, Zeng X, Cai M, Zhao D (2022) The MSI1 member *OsRBAP1* gene, identified by a modified MutMap method, is required for rice height and spikelet fertility. Plant Sci 320:111201. https://doi.org/10.1016/j.plantsci.2022.111201

Huerta-Cepas J, Szklarczyk D, Heller D, Hernández-Plaza A, Forslund SK, Cook H, Mende DR, Letunic I, Rattei T, Jensen LJ (2019) eggNOG 5.0: a hierarchical, functionally and phylogenetically annotated orthology resource based on 5090 organisms and 2502 viruses. Nucleic Acids Res 47(D1):309–314. https://doi.org/10.1093/nar/gky1085

Igari K, Endo S, Hibara K, Aida M, Sakakibara H, Kawasaki T, Tasaka M (2008) Constitutive activation of a CC-NB-LRR protein alters morphogenesis through the cytokinin pathway in *Arabidopsis*. Plant J 55(1):14–27. https://doi.org/10.1111/j.1365-313X.2008.03466.x

Ishida Y, Tsunashima M, Hiei Y, Komari T (2015) Wheat (*Triticum aestivum* L.) transformation using immature embryos. Methods Mol Biol 1223:199–209. https://doi.org/10.1007/978-1-4939-1695-5_15

Jiao Y, Wang Y, Xue D, Wang J, Yan M, Liu G, Dong G, Zeng D, Lu Z, Zhu X, Qian Q, Li J (2010) Regulation of *OsSPL14* by OsmiR156 defines ideal plant architecture in rice. Nature Genet 42(6):541–544. https://doi.org/10.1038/ng.591

Kebrom TH, Mullet JE (2015) Photosynthetic leaf area modulates tiller bud outgrowth in sorghum. Plant Cell Environ 38(8):1471–1478. https://doi.org/10.1111/pce.12500

Kebrom TH, Chandler PM, Swain SM, King RW, Richards RA, Spielmeyer W (2012) Inhibition of tiller bud outgrowth in the *tin* mutant of wheat is associated with precocious internode development. Plant Physiol 160(1):308–318. https://doi.org/10.1104/pp.112.197954

Kepinski S, Leyser O (2005) The *Arabidopsis* F-box protein TIR1 is an auxin receptor. Nature 435(7041):446–451. https://doi.org/10.1038/nature03542

Komatsu K, Maekawa M, Ujiie S, Satake Y, Furutani I, Okamoto H, Shimamoto K, Kyozuka J (2003) *LAX* and *SPA*: major regulators of shoot branching in rice. Proc Natl Acad Sci U S A 100(20):11765–11770. https://doi.org/10.1073/pnas.1932414100

Koumoto T, Shimada H, Kusano H, She K-C, Iwamoto M, Takano M (2013) Rice monoculm mutation *moc2*, which inhibits outgrowth of the second tillers, is ascribed to lack of a fructose-1, 6-bisphosphatase. Plant Biotechnol J 30(1):47–56. https://doi.org/10.5511/plantbiotechnology.12.1210a

Kumar L, Futschik ME (2007) Mfuzz: a software package for soft clustering of microarray data. Bioinformation 2(1):5–7. https://doi.org/10.6026/97320630002005

Li X, Qian Q, Fu Z, Wang Y, Xiong G, Zeng D, Wang X, Liu X, Teng S, Hiroshi F (2003) Control of tillering in rice. Nature 422(6932):618–621. https://doi.org/10.1038/nature01518

Li H, Handsaker B, Wysoker A, Fennell T, Ruan J, Homer N, Marth G, Abecasis G, Durbin R (2009) The sequence alignment/map format and SAMtools. Bioinformatics 25(16):2078–2079. https://doi.org/10.1093/bioinformatics/btp352

Li H (2013) Aligning sequence reads, clone sequences and assembly contigs with BWA-MEM. Genomics 1303:3997. https://doi.org/10.48550/arXiv.1303.3997.

Liu R, Hou J, Li H, Xu P, Zhang Z, Zhang X (2021) Association of *TaD14–4D*, a gene involved in strigolactone signaling, with yield contributing traits in wheat. Int J Mol Sci 22 (7). https://doi.org/10.3390/ijms22073748.

Livak KJ, Schmittgen TD (2001) Analysis of relative gene expression data using real-time quantitative PCR and the 2(-Delta Delta C(T)) Method. Methods 25(4):402–408. https://doi.org/10.1006/meth.2001.1262

Love MI, Huber W, Anders S (2014) Moderated estimation of fold change and dispersion for RNA-seq data with DESeq2. Genome Biol 15(12):1–21. https://doi.org/10.1186/s13059-014-0550-8

Manchikatla PK, Kalavikatte D, Mallikarjuna BP, Palakurthi R, Khan AW, Jha UC, Bajaj P, Singam P, Chitikineni A, Varshney RK, Thudi M (2021) MutMap approach enables rapid identification of candidate genes and development of markers associated with early flowering and enhanced seed size in Chickpea (Cicer arietinum L.). Front Plant Sci 12:688694. https://doi.org/10.3389/fpls.2021.688694

Mason MG, Ross JJ, Babst BA, Wienclaw BN, Beveridge CA (2014) Sugar demand, not auxin, is the initial regulator of apical dominance. Proc Natl Acad Sci U S A 111(16):6092–6097. https://doi.org/10.1073/pnas.1322045111

Matthes MS, Best NB, Robil JM, Malcomber S, Gallavotti A, McSteen P (2019) Auxin evodevo: conservation and diversification of genes regulating auxin biosynthesis, transport, and signaling. Mol Plant 12(3):298–320. https://doi.org/10.1016/j.molp.2018.12.012

McCormick RF, Truong SK, Mullet JE (2015) RIG: recalibration and interrelation of genomic sequence data with the GATK. G3-Genes Genomes Genet 5(4):655–665. https://doi.org/10.1534/g3.115.017012.

Michael Weaver L, Swiderski MR, Li Y, Jones JD (2006) The *Arabidopsis thaliana* TIR-NB-LRR R-protein, RPP1A; protein localization and constitutive activation of defence by truncated alleles in tobacco and *Arabidopsis*. Plant J 47(6):829–840. https://doi.org/10.1111/j.1365-313X.2006.02834.x

Pan YH, Chen L, Guo HF, Feng R, Lou QJ, Rashid MAR, Zhu XY, Qing DJ, Liang HF, Gao LJ, Huang CC, Zhao Y, Deng GF (2022) Systematic analysis of *NB-ARC* gene family in rice and functional characterization of *GNP12*. Front Genet 13:887217. https://doi.org/10.3389/fgene.2022.887217

Prykhozhij SV, Rajan V, Gaston D, Berman JN (2015) CRISPR multitargeter: a web tool to find common and unique CRISPR single guide RNA targets in a set of similar sequences. PLoS ONE 10(3):e0119372. https://doi.org/10.1371/journal.pone.0119372

Rabot A, Henry C, Ben Baaziz K, Mortreau E, Azri W, Lothier J, Hamama L, Boummaza R, Leduc N, Pelleschi-Travier S, Le Gourrierec J, Sakr S (2012) Insight into the role of sugars in bud burst under light in the rose. Plant Cell Physiol 53(6):1068–1082. https://doi.org/10.1093/pcp/pcs051

Rairdan GJ, Moffett P (2006) Distinct domains in the ARC region of the potato resistance protein Rx mediate LRR binding and inhibition of activation. Plant Cell 18(8):2082–2093. https://doi.org/10.1105/tpc.106.042747

Rairdan G, Moffett P (2007) Brothers in arms? Common and contrasting themes in pathogen perception by plant NB-LRR and animal NACHT-LRR proteins. Microbes Infect 9(5):677–686. https://doi.org/10.1016/j.micinf.2007.01.019

Shimizu-Sato S, Tanaka M, Mori H (2009) Auxin–cytokinin interactions in the control of shoot branching. Plant MolBiol 69(4):429–435. https://doi.org/10.1007/s11103-008-9416-3

Smith SM, Li J (2014) Signalling and responses to strigolactones and karrikins. Curr Opin Plant Biol 21:23–29. https://doi.org/10.1016/j.pbi.2014.06.003

Spielmeyer W, Richards RA (2004) Comparative mapping of wheat chromosome 1AS which contains the tiller inhibition gene (tin) with rice chromosome 5S. Theor Appl Genet 109(6):1303–1310. https://doi.org/10.1007/s00122-004-1745-2

Takagi H, Abe A, Yoshida K, Kosugi S, Natsume S, Mitsuoka C, Uemura A, Utsushi H, Tamiru M, Takuno S, Innan H, Cano LM, Kamoun S, Terauchi R (2013a) QTL-seq: rapid mapping of quantitative trait loci in rice by whole genome resequencing of DNA from two bulked populations. Plant J 74(1):174–183. https://doi.org/10.1111/tpj.12105

Takagi H, Uemura A, Yaegashi H, Tamiru M, Abe A, Mitsuoka C, Utsushi H, Natsume S, Kanzaki H, Matsumura H, Saitoh H, Yoshida K, Cano LM, Kamoun S, Terauchi R (2013b) MutMap-Gap: whole-genome resequencing of mutant F2 progeny bulk combined with *de novo* assembly of gap regions identifies the rice blast resistance gene *Pii*. New Phytol 200(1):276–283. https://doi.org/10.1111/nph.12369

Takagi H, Tamiru M, Abe A, Yoshida K, Uemura A, Yaegashi H, Obara T, Oikawa K, Utsushi H, Kanzaki E, Mitsuoka C, Natsume S, Kosugi S, Kanzaki H, Matsumura H, Urasaki N, Kamoun S, Terauchi R (2015) MutMap accelerates breeding of a salt-tolerant rice cultivar. Nat Biotechnol 33(5):445–449. https://doi.org/10.1038/nbt.3188

Takeda T, Suwa Y, Suzuki M, Kitano H, Ueguchi-Tanaka M, Ashikari M, Matsuoka M, Ueguchi C (2003) The *OsTB1* gene negatively regulates lateral branching in rice. Plant J 33(3):513–520. https://doi.org/10.1046/j.365-313x.2003.01648.x

Takken F, Tameling W (2009) To nibble at plant resistance proteins. Science 324(5928):744–746. https://doi.org/10.1126/science.1171666

Tanaka M, Takei K, Kojima M, Sakakibara H, Mori H (2006) Auxin controls local cytokinin biosynthesis in the nodal stem in apical dominance. Plant J 45(6):1028–1036. https://doi.org/10.1111/j.1365-313X.2006.02656.x

Wang K, Li M, Hakonarson H (2010) ANNOVAR: functional annotation of genetic variants from high-throughput sequencing data. Nucleic Acids Res 38(16):e164. https://doi.org/10.1093/nar/gkq603

Wang B, Smith SM, Li J (2018a) Genetic regulation of shoot architecture. Annu Rev Plant Biol 69:437–468. https://doi.org/10.1146/annurev-arplant-042817-040422

Wang H, Zhang Y, Sun L, Xu P, Tu R, Meng S, Wu W, Anis GB, Hussain K, Riaz A, Chen D, Cao L, Cheng S, Shen X (2018b) *WB1*, a regulator of endosperm development in rice, is identified by a modified MutMap method. Int J Mol Sci 19(8):2159. https://doi.org/10.3390/ijms19082159

Wang C, Tang S, Zhan Q, Hou Q, Zhao Y, Zhao Q, Feng Q, Zhou C, Lyu D, Cui L (2019) Dissecting a heterotic gene through GradedPool-Seq mapping informs a rice-improvement strategy. Nat Commun 10(1):1–12. https://doi.org/10.1038/s41467-019-11017-y

Wu T, Hu E, Xu S, Chen M, Guo P, Dai Z, Feng T, Zhou L, Tang W, Zhan L (2021) clusterProfiler 4.0: a universal enrichment tool for interpreting omics data. Innovation-Amsterdam 2(3):100141. https://doi.org/10.1016/j.xinn.2021.100141

Xie Z, Zhang Q, Xia C, Dong C, Li D, Liu X, Kong X, Zhang L (2023) Identification of the early leaf senescence gene ELS3 in bread wheat (Triticum aestivum L.). Planta 259(1):5. https://doi.org/10.1007/s00425-023-04278-x

Xing HL, Dong L, Wang ZP, Zhang HY, Han CY, Liu B, Wang XC, Chen QJ (2014) A CRISPR/Cas9 toolkit for multiplex genome editing in plants. BMC Plant Biol 14:327. https://doi.org/10.1186/s12870-014-0327-y

Xiong H, Zhou C, Fu M, Guo H, Xie Y, Zhao L, Gu J, Zhao S, Ding Y, Li Y (2022) Cloning and functional characterization of *Rht8*, a "Green Revolution" replacement gene in wheat. Mol Plant 15(3):373–376. https://doi.org/10.1016/j.molp.2022.01.014

Yang S, Hua J (2004) A haplotype-specific *Resistance* gene regulated by *BONZAI1* mediates temperature-dependent growth control in *Arabidopsis*. Plant Cell 16(4):1060–1071. https://doi.org/10.1105/tpc.020479

Yang F, Wang Q, Schmitz G, Müller D, Theres K (2012) The bHLH protein ROX acts in concert with RAX1 and LAS to modulate axillary meristem formation in *Arabidopsis*. Plant J 71(1):61–70. https://doi.org/10.1111/j.1365-313X.2012.04970.x

Yuan Y, Khourchi S, Li S, Du Y, Delaplace P (2023) Unlocking the multifaceted mechanisms of bud outgrowth: advances in understanding shoot branching. Plants-Basel 12(20):3628–3652. https://doi.org/10.3390/plants12203628

Zhang B, Liu X, Xu W, Chang J, Li A, Mao X, Zhang X, Jing R (2015) Novel function of a putative *MOC1* ortholog associated with spikelet number per spike in common wheat. Sci Rep 5:12211. https://doi.org/10.1038/srep12211

Zhao B, Wu TT, Ma SS, Jiang DJ, Bie XM, Sui N, Zhang XS, Wang F (2020) *TaD27-B* gene controls the tiller number in hexaploid wheat. Plant Biotechnol J 18(2):513–525. https://doi.org/10.1111/pbi.13220